

ORIGINAL ARTICLE

Open Access

Tailoring the photocatalytic reaction rate of a nanostructured TiO₂ matrix using additional gas phase oxygen

Mohammed Jasim Uddin^{1,4*}, Md Mohibul Alam¹, Md Akhtarul Islam¹, Sharmin Rahman Snigda¹, Sreejon Das¹, Mohammed Mastabur Rahman¹, Md Nizam Uddin², Cindy A Morris³, Richard D Gonzalez^{4*}, Ulrike Diebold⁵, Tarik J Dickens⁶ and Okenwa I Okoli⁶

Abstract

Nanostructured TiO₂ was synthesized by the sol–gel method. The titania was supported on nanoporous poly (styrene-co-divinylbenzene) (PS). The samples were characterized by several techniques (scanning electron microscopy, energy-dispersive spectroscopy, X-ray diffraction, and ultraviolet–visible spectroscopy). Three types of TiO₂ samples were prepared using various temperatures and were studied for the photocatalytic degradation of methylene blue. The photocatalytic efficiency of TiO₂ was observed to increase by activating the TiO₂ surface using nanoporous PS. The photocatalytic performance of the synthesized samples showed a higher performance using molecular O₂, which was purged through the reactor.

Keywords: Titanium dioxides (TiO₂), Sol–gel method, Photocatalyst, Poly(styrene-co-divinylbenzene), Oxygen

Background

The photocatalytic activity of TiO₂ is widely used in many fields, such as microorganism disinfection [1], medical treatment [2], environmental purification [3], and photovoltaic cells [4,5]. It was reported that the physical characteristics of TiO₂, including crystallization, grain size, morphology, specific surface area, surface state, and porosity influence the photocatalytic activity of TiO₂ [6-8]. TiO₂ can be synthesized into various shapes, e.g., nanoporous materials, nanoparticles, nanowires, nanorods, nanotubes, and nanofibers using different preparation methods, e.g., sol–gel, hydrothermal, solvothermal, microemulsion, and vapor deposition [9-11]. Following this advancement, TiO₂ plays an important role as a photocatalyst in many applications, such as fog proof and self-cleaning textiles, antibacterial textiles, antiviral textiles, self-cleaning glass, and water treatment, including dye removal from industrial wastewater

[12-15]. Photocatalytic oxidation is one of the most promising techniques used in the remediation of organic micropollutants because it is highly efficient in mineralization using sunlight as an energy source [16]. TiO₂ nanoparticles are effective for the photocatalytic degradation of various organic contaminants in water. However, its practical use is difficult for filtration and the recovery of small TiO₂ particles [17]. TiO₂ has proven to be an excellent photocatalytic material, which undergoes complete mineralization under UV exposure [18]. Redox reactions of environmental interest are initiated on a TiO₂ surface by trapped electron holes following bandgap excitation. Significant effort has been made in the last 20 years to modify TiO₂ particles, which can be activated under visible light irradiation ($\lambda > 400$ nm) [19]. Titanium dioxide has been extensively used, either as a thin film or as a submicron powder, in electronic or optical devices as well as in pigments or catalysts. The photocatalytic activity of TiO₂ can be improved by using it as carbon, carbon nanotubes, fullerenes, or graphene composites to enhance the photocatalytic activity as opposed to using TiO₂ alone [20-23]. It was previously reported that the incorporation of nanoporous

* Correspondence: muddin@fsu.edu; gonzo@tulane.edu

¹Department of Chemical Engineering and Polymer Science, Shahjalal University of Science and Technology, Sylhet 3114, Bangladesh

⁴Department of Chemical and Biomolecular Engineering, Tulane University, New Orleans, LA 70118, USA

Full list of author information is available at the end of the article

poly(styrene-*co*-divinylbenzene) (PS) during the synthesis of TiO₂ has positive effects on surface morphology [24].

In the present study, TiO₂ powders were synthesized from titanium isopropoxide, Ti(O-C₃H₇)₄ (referred to hereafter as TIP), in the presence of nanoporous PS, at room temperature and atmospheric pressure. Under such conditions, nanosized particles (20 to 60 nm) are partly crystallized in the anatase phase. The aims of our study are (a) to enhance the activity of the surface sites using PS as a support, (b) to check the photocatalytic activity of synthesized TiO₂ using methylene blue (MB), (c) to investigate the photocatalytic reaction kinetics using molecular oxygen that passes through the reactor, and (d) to investigate the photocatalytic degradation kinetics using several mathematical models. The addition of molecular oxygen in the photocatalytic reactor increases the degradation performance over that observed in the absence of oxygen in the reactor. The solution contains some dissolved oxygen that can also interact with TiO₂ under illumination. However, superior activity is observed through the addition of excess oxygen. This photocatalytic degradation method is novel because a stream of natural air is passed through the reactor in order to increase the reaction rate. The photocatalytic activity of nanocrystalline TiO₂ modified with PS was prepared using a one-step sol-gel process and monitored by measuring the photocatalytic degradation of absorbed MB. This was compared to that observed using P25.

Methods

Materials

All graded chemicals, titanium(IV) isopropoxide (Ti(O-C₃H₇)₄), methylene blue (Merck, Darmstadt, Germany), 2-propanol (Sigma-Aldrich, St. Louis, MO, USA), and poly(styrene-*co*-divinylbenzene) were used as received. The cross-linked PS used in these experiments is a copolymer resin commercialized by Aldrich in the form of 300- to 800- μ m beads. The polymer presents a BET surface area of 1,000 m² g⁻¹, as evaluated by N₂ adsorption at 77 K, and a pore size distribution centered at approximately 16 Å [25]. The water was double distilled and produced in our laboratory. P25 (Degussa Germany) was used as a standard photocatalyst material (TiO₂) throughout this study.

Synthesis of TiO₂ supported on PS using the sol-gel process

Nanostructured TiO₂ was prepared using sol-gel chemistry methods. The synthesis reactor consists of a three-necked round-bottom reactor flask equipped with a vertical condenser fitted to the middle neck. A separatory funnel was connected to one of the two side necks. Deionized water (12.24 ml) was added slowly to 51.19 ml of isopropanol under vigorous stirring for 20 min.

After adding TIP, isopropanol, water, and nanoporous PS (2 g) were added to the bottle, and the solution was vigorously stirred for 24 h. Another batch was prepared following the previous steps with the exception of PS. Following a 24-h period, the solvent was dried using a vacuum evaporator and the white powder was calcined at temperatures of 450°C, 550°C, and 650°C in an electric muffle furnace (JSMT-30T, JEOL Ltd., Seoul, South Korea). The photocatalytic performance has been compared with that of P25 as the standard photocatalyst.

Characterization techniques

Scanning electron microscopy (SEM) was performed using a Hitachi S-4800 field emission scanning electron microscope (Hitachi Ltd., Chiyoda-ku, Japan) operated at 3 kV to characterize the TiO₂ nanostructure. Energy-dispersive spectroscopy (EDS) spectra were recorded using a high-resolution transmission electron microscope (TEM), JEOL 2010, operated at 200 kV and equipped with an EDS microanalysis system (Oxford Instruments, Abingdon, UK).

The X-ray diffraction (XRD) patterns were obtained using a Bruker D-5000 diffractometer (Bruker AXS, Inc., Madison, WI, USA) equipped with Cu K α radiation with a wavelength of 1.5418 Å. The accelerating voltage and the applied current were 45 kV and 40 mA, respectively.

Photocatalytic experiment

The photocatalytic activity of titanium dioxides was studied by exposing the TiO₂ sample, which contained a dye such as MB, to solar-like conditions. For photocatalytic reactions, the irradiation was carried out in a solution at 308 K, using a SOL 21500 lamp (SOL, Inc., Palm City, FL, USA). The SOL bulb yields a spectrum very similar to that of the natural sunlight ranging from ultraviolet to infrared radiation (approximately 295 to 3,000 nm). For this purpose, an aqueous solution (0.05% w/v) of reagent-grade MB was prepared for the impregnation of reference and synthesized TiO₂. The same amount (0.5 g) of each TiO₂ sample was inserted under very mild stirring in the same amount of solution (50 ml) and remained there for 2 to 3 min to complete the mixing. The solution was then placed under the solar-like light (50 to 60 mW/cm²). Continuous stirring (200 rpm) and natural air flow (50 ml/min, 20 vol.% oxygen) were maintained during the photocatalytic reaction. The gas was passed underneath the reactor using a porous filter media (mesh size, 200), which dissipates the gas molecules (0.027 g O₂ min⁻¹ g⁻¹ TiO₂) to the MB solution. The photocatalytic decomposition reaction was monitored with an ultraviolet-visible (UV-vis) spectrophotometer (UV-1650, Shimadzu Corporation, Nakagyo-ku, Kyoto, Japan) in the transmission mode by investigating the evolution of the absorbed MB band upon light exposure.

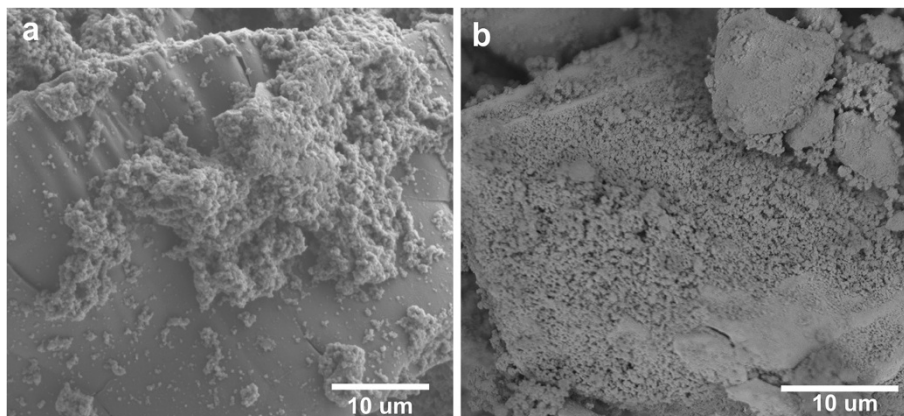


Figure 1 SEM images of TiO₂ particles. Prepared (a) without and (b) with the presence of nanoporous PS using the sol-gel process.

Degradation-diffusion kinetics

Four kinetic models were used to investigate the data that were obtained during the photodegradation of the catalyst [26-28]:

1. The zero-order model describes the photocatalytic kinetic process and can be generally expressed as

$$C_t - C_0 = -kt \quad (1)$$

2. The first-order model expresses the photocatalytic degradation rate which is dependent on the amount of MB in the TiO₂ matrix and can be written as

$$\log (C_t/C_0) = kt \quad (2)$$

3. The parabolic diffusion model elucidates the diffusion-controlled photodegradation of MB on the TiO₂ surface. The equation can be written as

$$\frac{(1 - C_t/C_0)}{t} = kt^{-\frac{1}{2}} + \alpha \quad (3)$$

4. The modified Freundlich model explains experimental data on molecular ion exchange and diffusion-controlled processes using the following equation:

$$\frac{C_0 - C_t}{C_0} = kt^b \quad (4)$$

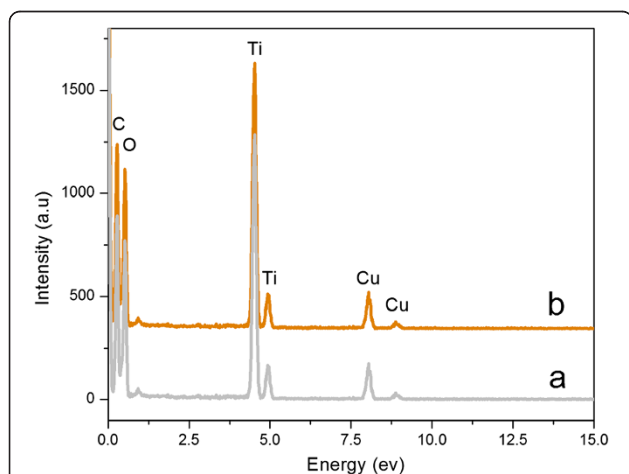


Figure 2 EDS spectrum of individual nanoparticles joined together to form a TiO₂ matrix. Synthesized (curve a) without and (curve b) with the presence of nanoporous PS. The copper (Cu) and carbon (C) peaks are from the TEM grids.

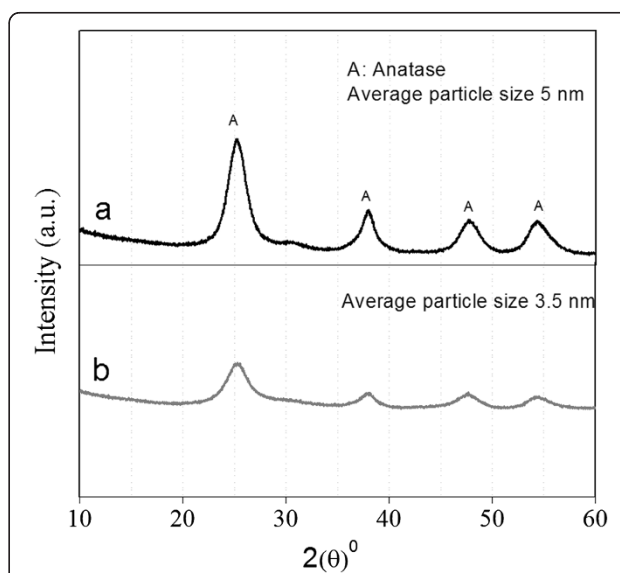


Figure 3 XRD patterns of TiO₂. Synthesized (curve a) without and (curve b) with the presence of nanoporous PS, calcined at 550°C. 'A' indicates the anatase phase of TiO₂.

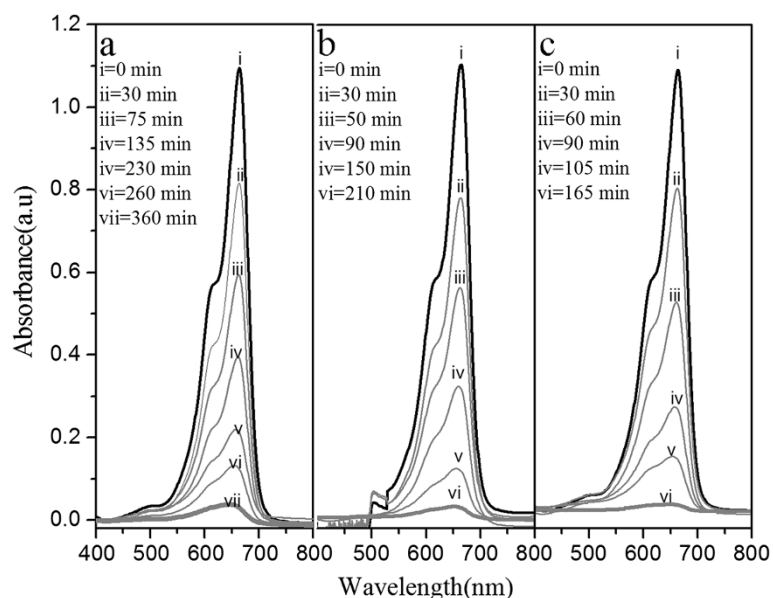


Figure 4 UV-vis spectral changes of the photocatalytic degradation of MB on TiO₂. Calcined at (a) 450°C, (b) 550°C, and (c) 650°C.

In these equations, C_0 and C_t represent the concentration of MB in the system at time 0 and t , respectively, k is the corresponding reaction rate constant, and a and b are fitting parameters whose chemical significance are not clearly resolved [29].

Results and discussion

SEM and EDS analyses

Field emission SEM images of the synthesized TiO₂ nanoparticles prepared using the sol-gel chemistry

method are shown in Figure 1a,b. Figure 1a,b shows the TiO₂ synthesized without and with support of PS, respectively. Figure 1a shows that the TiO₂ aggregates are lumped together along with a portion of loose particles attached together, while Figure 1b shows a general porous structure with a large number of pores of very small dimensions. This feature suggests that the porous nature of PS-supported TiO₂ potentially results in a high surface area and preferentially enable the particles to adsorb organic molecules [30] or pollutants

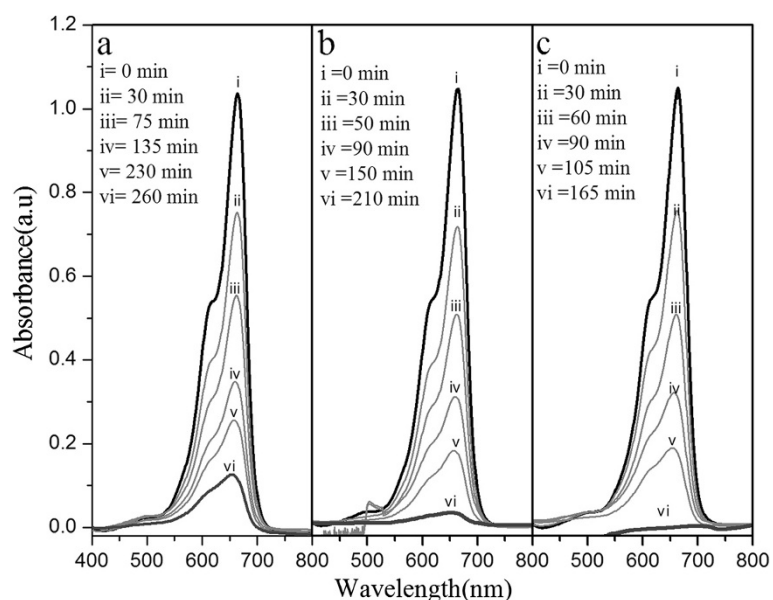
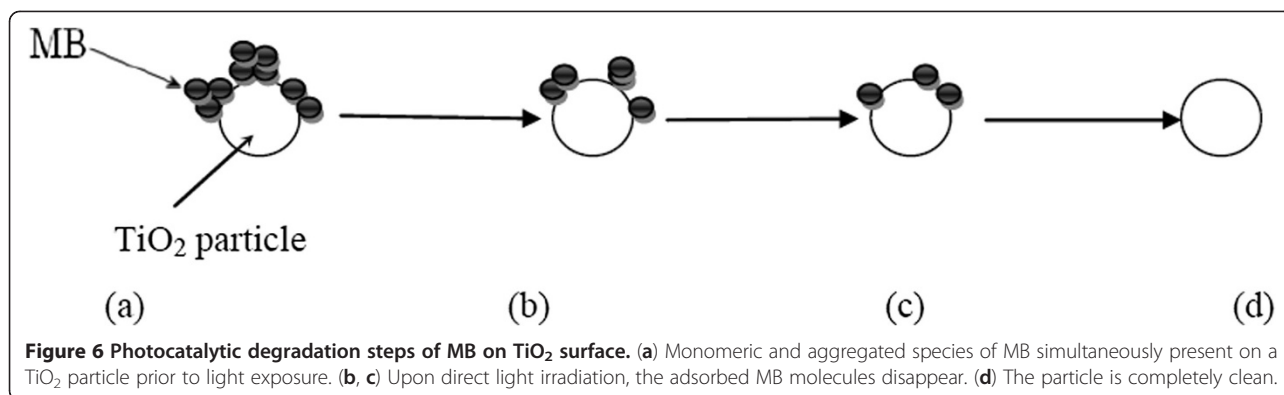


Figure 5 UV-vis spectral changes in the photocatalytic degradation of MB under solar-like irradiation on TiO₂. Synthesized on supported PS and calcined at (a) 450°C, (b) 550°C, and (c) 650°C.



adhered to the surface [31,32]. However, the morphology of the PS-supported TiO₂ matrix shows the uniformity of the aggregates that consist of individual particles in the nanoscale range, in agreement with XRD analysis (*vide infra*). EDS was performed by TEM analysis (figure not shown for the sake of brevity). Each element is distinctly identified on the resulting spectrum. Figure 2 shows that the matrix consisted of only titanium (Ti) and oxygen (O). This implies that the synthesized nanostructured TiO₂ is free of contaminants.

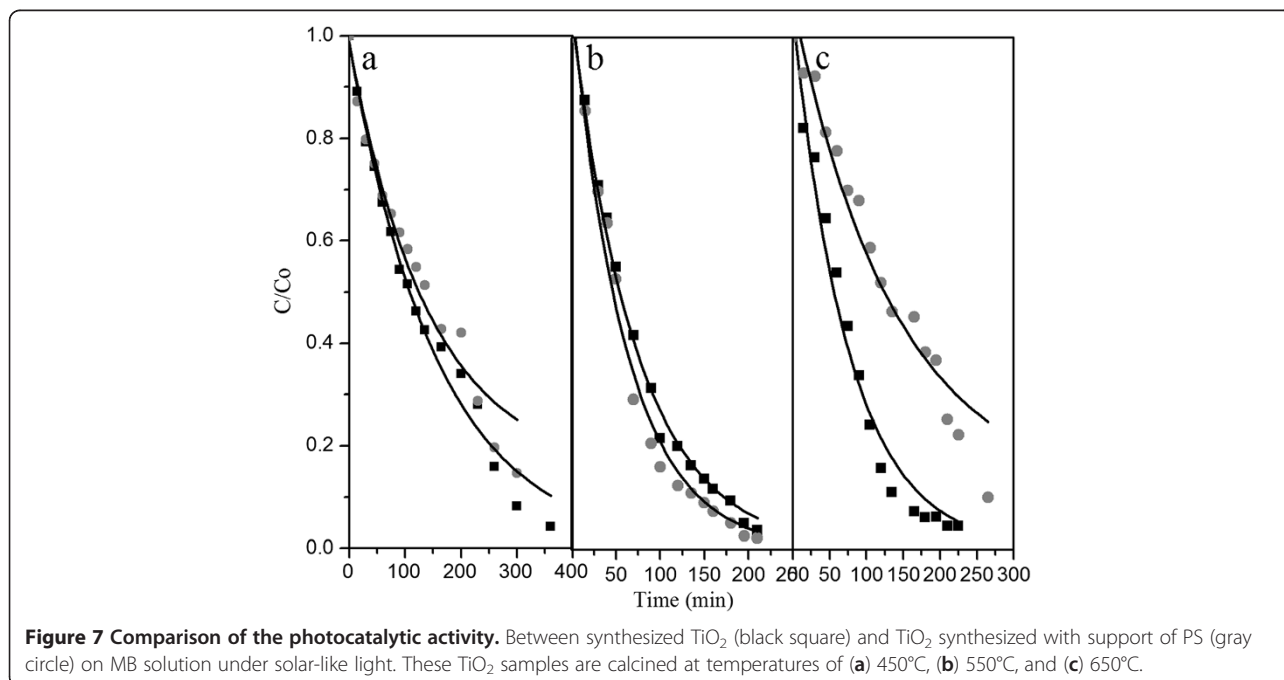
XRD analysis

The XRD patterns of synthesized TiO₂ calcined at 550°C are in Figure 3 (curves a and b). Curves a and b report three broad peaks and one intense peak at 37.95°, 47.68°, 54.31°, and 25.19°, respectively, which

constitute the XRD pattern of the anatase phase of TiO₂ [12]. No additional peaks belonging to rutile phases were observed. The widths of the peaks associated with the TiO₂ phase suggest that the size of the particles is quite small. From the full width at half maximum (FWHM) of the peaks at 25.1° and 38.01° and using Scherrer's equation, $L_c = K\lambda/(\beta \cos \theta)$ [33] (where λ is the X-ray wavelength, β is the FWHM been assumed to be 0.9), an average particle size of approximately 3 to 5 nm is calculated. In addition, the PS-supported TiO₂ shows a particle size of approximately 3.5 nm, which is indicative of a large surface area and is consistent with the SEM analysis described above.

Photocatalytic performance

The photocatalytic activity of TiO₂ nanostructures was carried out at room temperature using solar-like



radiation. To compare the photocatalytic activity, the same concentration and conditions were maintained during the experiment. The spectra were collected for the prepared TiO₂ samples calcined at different temperatures. The UV-vis spectra obtained in solution before (curve i) and after illumination (curves ii to vii) are reported in Figures 4 and 5. Figure 4 shows the photocatalytic activity of TiO₂ toward MB, while Figure 5 shows the photocatalytic activity of the TiO₂ synthesized with support of PS towards MB. The spectra show the consequence of the photocatalytic degradation of MB using a batch reactor under solar-like light conditions having a maximum absorbance at 664 nm.

From Figures 4 and 5, it can be observed that the complex absorption band in the 500 to 700 nm (20,000 to 12,000 cm⁻¹) interval due to the presence of MB changes rapidly because dispersed TiO₂ particles promote catalytic photodegradation (curves i to vii). According to the published literature [12], the bands at 600 nm (16,400 cm⁻¹) and 664 nm (15,400 cm⁻¹) are assigned to monomer and aggregates, respectively, the latter to dimeric and trimeric MB species (Figure 6). Under light exposure, the aggregates or dimers and trimers of MB disappear first, followed by the monomeric species.

Figure 7a,b,c shows that the photocatalytic degradation of the sample calcined at a temperature of 550°C performs better on MB than those of the samples treated at 450°C and 650°C. It should be noted that the sample calcined at 450°C has a certain portion of hydrogen titanate, while the sample calcined at 650°C contains a higher concentration of TiO₂ in the rutile phase [34], which are less efficient in photocatalytic degradation of organics (Figure 7). Among them, the sample supported on PS and calcined at 550°C shows a better performance on the photocatalytic degradation of MB which possibly is indicative of high surface area, which could possibly be associated with a larger number of active surface sites, produced during the combustion of supported PS with TiO₂. This observation is in agreement with SEM and XRD analyses. This sample shows a similar photocatalytic behavior in comparison to P25 that is the most effective photocatalyst (*vide infra*). Four types of degradation kinetic models (zero-order, first-order, parabolic diffusion, and modified Freundlich model) are applied and calculated at the corresponding linear correlation coefficients (R^2) (Figure 8; Table 1). Here, the zero, parabolic diffusion, and modified Freundlich models are not suitable to explain the entire system, clearly the data points that do not form a

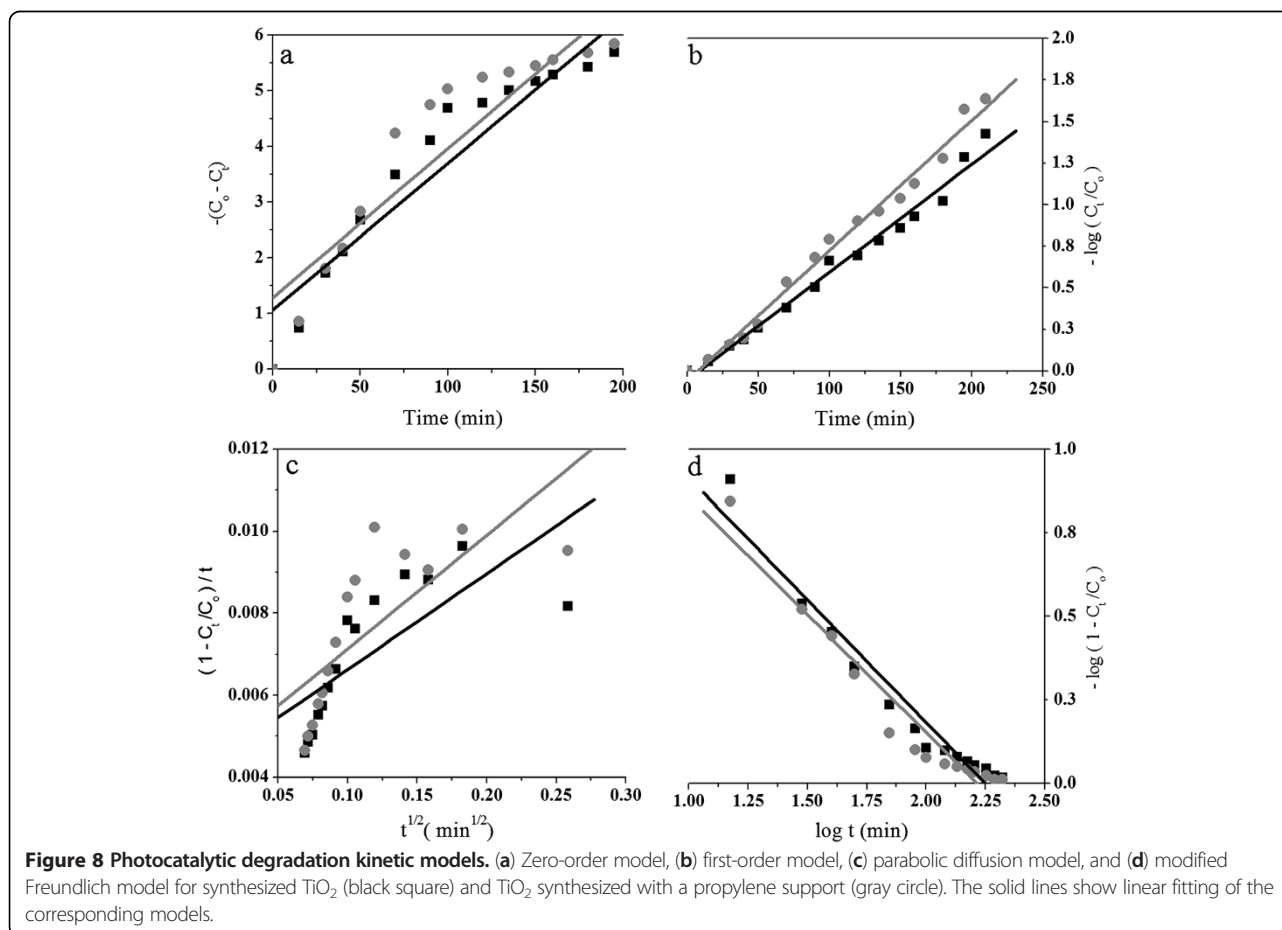


Table 1 R² of photocatalytic kinetic models applied to bare TiO₂ and TiO₂ synthesized with PS support

Photocatalytic degradation kinetic models	Synthesized TiO ₂		TiO ₂ synthesized with support of PS	
	R ²	k	R ²	k
Zero-order model	0.89742	0.02637	0.84587	0.02679
First-order model	0.98321	0.00649	0.98754	0.00784
Parabolic diffusion model	0.55254	0.02339	0.56175	0.0277
Modified Freundlich model	0.95004	0.73221	0.93236	0.70542

straight line (Figure 8a,c,d). The other model indicates a better fit (Figure 8b). The correlation coefficient lies between 0.552 and 0.932 for the zero-order, parabolic diffusion, and modified Freundlich models, while for the first-order model, they are between 0.983 and 0.987. These data indicate that the first-order model fits the experimental photodegradation data quite well. A detailed examination of the data point distribution in Figure 8 suggests that the entire photocatalytic degradation process consists of monoliner models. This result suggests that (1) the system is adsorption-desorption-controlled and (2) the photocatalytic degradation is occurring at the TiO₂ surface.

Figure 9 shows the photocatalytic degradation kinetics of MB using an oxygen flow to the reactor. The photocatalytic activity of the different samples compared to that of the control experiment (Figure 9, dotted line), which was performed

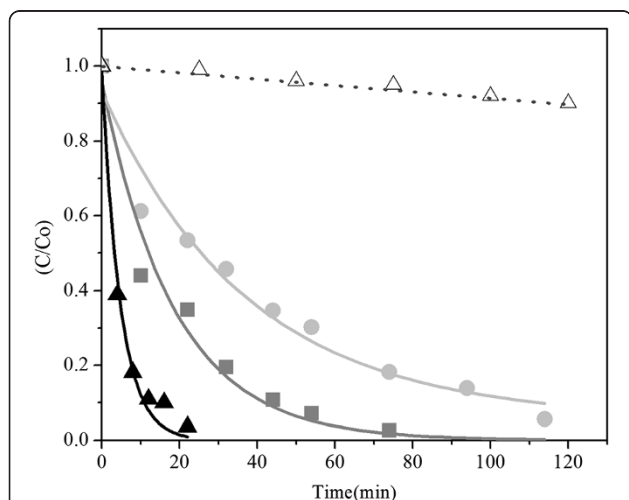
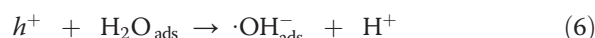


Figure 9 Photocatalytic activity. Using synthesized TiO₂ (gray circle), TiO₂ synthesized with support of PS (black square), and P25 (black triangle) under controlled air supplied to the reactor. The dot line represents (white triangle) the photodegradation of MB in aqueous solution without the presence of TiO₂ under same irradiation.

in the absence of TiO₂ and oxygen, confirms that our catalysts are capable of photocatalytic degradation. Figure 9 shows that photodegradation of MB without the presence of any TiO₂ catalyst is negligible. Notice that using the additional oxygen flow, the MB molecules degrade at least three times more

rapidly than that of the photocatalytic system carried out without oxygen flow (Figures 7 and 9). It is known that the degradation of stains by a UV/TiO₂ process proceeds in the presence of a humid atmosphere [12]. Probably, the dissolved oxygen supplies the oxidant required for the preferred photocatalytic reaction. These results suggest that the stain molecules are favorably degraded under solar-like light on the TiO₂ surface in the presence of oxygen molecules.

The illumination of TiO₂ under ultraviolet light changes the energy state of electrons from the valence band to the conduction band to give electron-hole pairs. The holes at the TiO₂ valence band can oxidize water or hydrolyze to produce hydroxyl groups. The hydroxyl radical is a powerful oxidizing agent that attacks organic compounds forming intermediates (*I*). These intermediates react with hydroxyl radicals to produce the final product (*P*). Hydroxyl radicals can also be consumed by inactive species [35-37]:



In addition, we can arrange the photocatalytic reaction to proceed by an additional reaction as follows:



The presence of molecular oxygen speeds up the potential reactions of photon energy conversion to active species which take part sustainably in organic/stain photodegradation [38]. Photocatalytic reactions in the solid or liquid phase should contain either adjacent gaseous or dissolved oxygen, respectively, to complete the photodegradation process. This phenomenon is in agreement with the dependence of the photodegradation ability of the TiO₂ conduction band with the LUMO level of the adsorbed molecule (band alignment) which has already been observed [10,12]. From these data, it is evident that (1) supported PS particles promote the photocatalytic activity of TiO₂ synthesized using the sol-gel

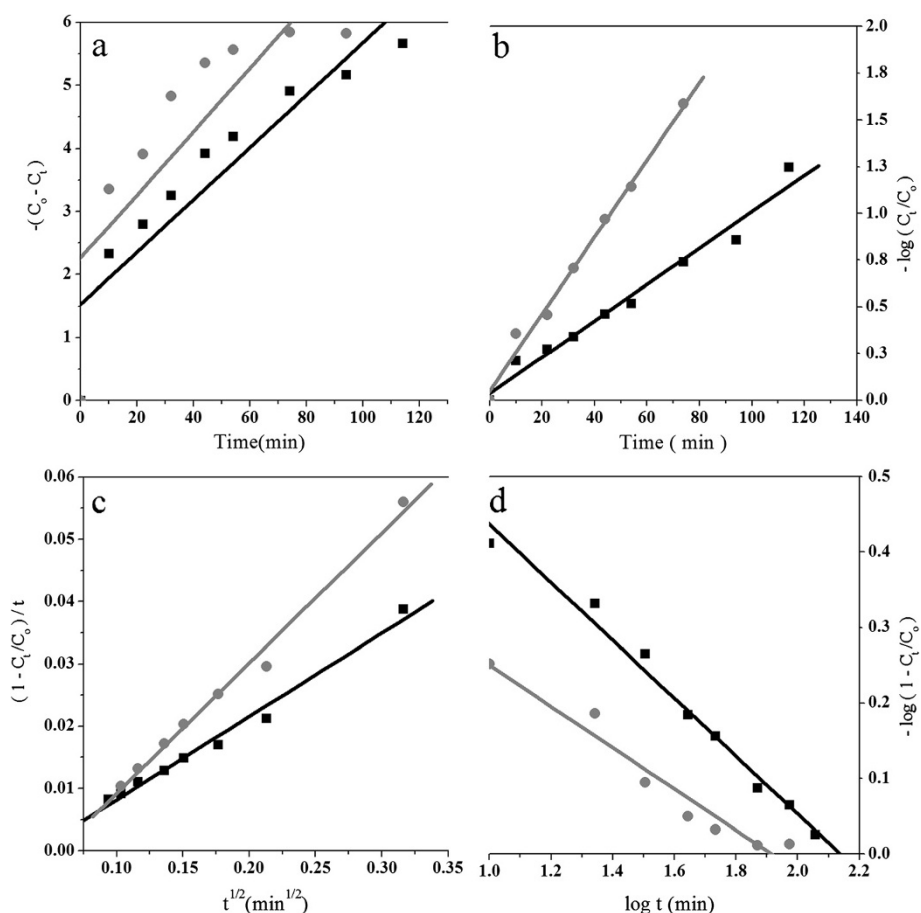


Figure 10 Photocatalytic kinetic models of the system with a controlled air supply. (a) Zero-order model, (b) first-order model, (c) parabolic diffusion model, and (d) modified Freundlich model for synthesized TiO_2 (black square) and TiO_2 synthesized with support of PS which was calcined at temperature of 550°C (gray circle).

process and (2) the high surface area associated with the small particle size ensures a favorable condition for rapid degradation.

Four types of kinetic models (zero-order, first-order, parabolic diffusion, and modified Freundlich model; Figure 10) are also applied and calculated at the corresponding reaction rate constant and linear correlation coefficient (R^2 ; Table 2). Here, the zero-order model is not suitable to explain the entire system, which is reflected by modeling data that do not form a straight line (Figure 10a). The other three models fit the data much better ($R^2 = 0.974$ to 0.990 ; Figure 10b,c,d). A detailed examination of

data point distribution in Figure 10 suggests that the whole photocatalytic degradation process consists of monolinear modeling. The modified Freundlich model describes heterogeneous diffusion from the flat surfaces to the solvent using a composition gradient. This result suggests that (1) the system is adsorption-desorption-controlled and (2) the photocatalytic degradation of the dye molecules are occurring on the TiO_2 surface before leaving (desorption) the surface patches [39-41].

Table 2 shows the photocatalytic degradation performance of the photocatalyst on MB with the presence of solar-like light and controlled air supply. The photocatalytic

Table 2 R^2 of photodegradation kinetic models (with controlled air supply) applied to bare and synthesized TiO_2

Degradation decomposition kinetic models	Synthesized TiO_2		TiO_2 synthesized with support of PS	
	R^2	k	R^2	k
Zero-order model	0.84348	0.04148	0.66297	0.0502
First-order model	0.97443	0.00973	0.991	0.0206
Parabolic diffusion model	0.98359	0.13374	0.99006	0.2090
Modified Freundlich model	0.98341	0.27344	0.94383	0.38394

removal (degradation) efficiency of bare TiO₂ ($k_{\text{first-order}} = 0.000973$ and $k_{\text{modified Freundlich model}} = 0.2734$) in comparison to TiO₂ synthesized with a PS support ($k_{\text{first-order}} = 0.0206$ and $k_{\text{modified Freundlich model}} = 0.3839$) is much less. The lower degradation rate constant in synthesized TiO₂ in general could be due to scattering phenomena, where active sites on the surface of the catalyst do not bring more electron-hole pair generation and therefore a decrease in the degradation rate occurs [42]. It can be concluded that TiO₂ synthesized on a PS support follows a first-order photocatalytic MB degradation, and the reaction rate ($k_{\text{first-order}} = 0.0206$ and $k_{\text{modified Freundlich model}} = 0.38394$) is greater for the system in which molecular oxygen is supplied as an additional oxidant for photoenergy conversion.

Conclusions

Nanostructured TiO₂ has been synthesized using a sol-gel chemistry method with the support of nanoporous PS. The photocatalyst shows better performance when additional molecular oxygen is supplied during the photocatalytic degradation process. It can be concluded that the photocatalytic reaction could be forwarded with a higher rate of reaction and photodegradation performance by supplying oxygen (O₂) molecules to the solution. These results demonstrate that the TiO₂ synthesized could be sustainably used for the treatment of industrial wastewater, especially that which contains organic dyes, to protect the environment.

Competing interests

The authors declare that they have no competing interests.

Authors' contributions

SRS, MMA, and SD participated in the design and carried out the experiment. MJU, UD, RDG, MAI, MMR, MNU, and CAM participated in experimental plan and drafted the manuscript. UD, RGD, TD, and OIO participated in kinetic modeling with overall supervision and coordination of the study. All authors read and approved the final manuscript.

Acknowledgments

This work was supported by a Research Enhancement Grant from Tulane University. SRS acknowledges the research fellowship program of Shahjalal University of Science and Technology.

Author details

¹Department of Chemical Engineering and Polymer Science, Shahjalal University of Science and Technology, Sylhet 3114, Bangladesh. ²Department of Chemistry, Shahjalal University of Science and Technology, Sylhet 3114, Bangladesh. ³Department of Microbiology and Immunology, Tulane University, New Orleans, LA 70118, USA. ⁴Department of Chemical and Biomolecular Engineering, Tulane University, New Orleans, LA 70118, USA. ⁵Department of Physics, Tulane University, New Orleans, LA 70118, USA. ⁶Department of Industrial and Manufacturing Engineering, FAMU-FSU College of Engineering, Tallahassee, FL 32310, USA.

Received: 27 July 2012 Accepted: 26 February 2013

Published: 21 March 2013

References

1. Sunada, K, Kikuchi, Y, Hashimoto, K, Fujishima, A: Bactericidal and detoxification effects of TiO₂ thin film photocatalysts. *Environ. Sci. Technol.* **32**, 726 (1998)
2. Cai, R, Kubota, Y, Shuin, T, Hashimoto, K, Fujishima, A: Induction of cytotoxicity by photoexcited TiO₂ particles. *Cancer. Res.* **52**, 2346 (1992)
3. Hoffmann, MR, Martin, ST, Choi, W, Bahnemann, DW: Environmental applications of semiconductor photocatalysis. *Chem. Rev.* **95**, 69 (1995)
4. O'Regan, B, Gratzel, M: A low-cost, high-efficiency solar cell based on dye-sensitized colloidal TiO₂ films. *Nature.* **353**, 737 (1991)
5. Liu, Y, Li, M, Wang, H, Zheng, J, Xu, H, Ye, Q, Shen, H: J. Phys. D: Synthesis of TiO₂ nanotube arrays and its application in mini-3D dye-sensitized solar cells. *Appl. Phys.* **43**, 205103 (2010)
6. Yu, J, Wang, G, Cheng, B, Zhou, M: Effects of hydrothermal temperature and time on the photocatalytic activity and microstructures of bimodal mesoporous TiO₂ powders. *App. Catal. B: Environ.* **69**, 171 (2007)
7. Ohtani, B, Ogawa, Y, Nishimoto, S: Photocatalytic activity of amorphous-anatase mixture of titanium (IV) oxide particles suspended in aqueous solutions. *J. Phys. Chem. B* **101**, 3746 (1997)
8. Subramanian, V, Wolf, EE, Kamat, PV: Catalysis with TiO₂/gold nanocomposites. *J. Am. Chem. Soc.* **126**, 4943 (2004)
9. Chen, X, Rao, SS: Synthesis of titanium dioxide (TiO₂) nanomaterials. *J. Nanosci. Nanotechnol.* **6**, 906 (2006)
10. Stathatos, E, Lianos, P, Monte, FD, Levy, D, Tsiourvas, D: Formation of TiO₂ and their deposition as thin films on glass substrates. *Langmuir.* **13**, 4295 (1997)
11. Yue, Y, Gao, Z: Synthesis of mesoporous TiO₂ with a crystalline framework. *Chem. Commun.* **18**, 1755 (2000)
12. Uddin, MJ, Cesano, F, Bonino, F, Bordiga, S, Spoto, G, Scarano, D, Zecchina, A: Photoactive TiO₂ films on cellulose fibres: synthesis and characterization. *J. Photochem. Photobiol. A-Chem.* **189**, 286 (2007)
13. Uddin, MJ, Cesano, F, Scarano, D, Bonino, F, Agostini, G, Spoto, G, Bordiga, S, Zecchina, A: Cotton textile fibres coated by Au/TiO₂ films: synthesis, characterization and self cleaning properties. *J. Photochem. Photobiol. A-Chem.* **199**, 64 (2008)
14. Herrmann, JM, Tahiri, H, Aitlchou, Y, Lassaletta, G, GonzalezElipe, AR, Fernandez, A: Appl. Characterization and photocatalytic activity in aqueous medium of TiO₂ and Ag-TiO₂ coatings on quartz. *Catal. B-Environ.* **13**, 219 (1997)
15. Belfroid, A, Van Velzen, M, van der Horst, B, Vethaak, D: Occurrence of bisphenol A in surface water and uptake in fish: evaluation of field measurements. *Chemosphere.* **49**, 97 (2002)
16. Ollis, DF, Pelizzetti, E, Serpone, N: Photocatalyzed destruction of water contaminants. *Environ. Sci. Technol.* **25**, 1522 (1991)
17. Guo, C, Ge, M, Liu, L, Gao, G, Feng, Y, Wang, Y: Directed synthesis of mesoporous TiO₂ microspheres: catalysts and their photocatalysis for bisphenol A degradation. *Environ. Sci. Technol.* **44**, 419 (2009)
18. Fox, MA, Dulay, MT: Heterogeneous photocatalysis. *Chem Rev* **93**, 341 (1993)
19. Choi, J, Park, H, Hoffmann, MR: Effects of single metal-ion doping on the visible-light photoreactivity of TiO₂. *J. Phys. Chem. C.* **114**, 783 (2009)
20. Woan, K, Pyrgiotakis, G, Sigmund, W: Photocatalytic carbon-nanotube-TiO₂ composites. *Adv. Mater.* **21**, 2233 (2009)
21. Xu, YJ, Zhuang, YB, Fu, XZ: New insight for enhanced photocatalytic activity of TiO₂ by doping carbon nanotubes: a case study on degradation of benzene and methyl orange. *J. Phys. Chem. C.* **114**, 2669 (2010)
22. Oh, WC, Jung, AR, Ko, WB: Preparation of fullerenes/ TiO₂ composite and its photocatalytic effect. *J. Ind. Eng. Chem.* **13**, 1208 (2007)
23. Yan, Z, Zi-Rong, T, Xianzhi, F, Yi-Jun, X: TiO₂-graphene nanocomposites for gas-phase photocatalytic degradation of volatile aromatic pollutant: is TiO₂-graphene truly different from other TiO₂-carbon composite materials. *J. Am. Chem. Soc.* **4**, 7303 (2010)
24. Li, Y, Sun, Z, Zhang, J, Zhang, K, Wang, Y, Wang, Z, Chen, X, Zhu, S, Yang, B: Polystyrene@TiO₂ core-shell microsphere colloidal crystals and nonspherical macro-porous materials. *J. Colloid. Int. Sci.* **325**, 567 (2008)
25. Chavan, S, Vitillo, JG, Uddin, MJ, Bonino, F, Lamberti, C, Groppo, E, Lillerud, K-P, Bordiga, S: Functionalization of UiO-66 metal-organic framework and highly cross-linked polystyrene with Cr(CO)₃: in situ formation, stability, and photoreactivity. *Chem. Mater.* **22**, 4602 (2010)
26. Barrow, GM: Physical Chemistry. McGraw-Hill, Boston (1996)
27. Kodama, T, Harada, Y, Ueda, M, Shimizu, K, Shuto, K, Komarneni, S: selective exchange and fixation of strontium ions with ultrafine Na-4-mica. *Langmuir.* **17**, 4881 (2001)
28. Yang, J-H, Han, Y-S, Park, M, Park, T, Hwang, S-J, Choy, J-H: New inorganic-based drug delivery system of indole-3-acetic acid-layered metal hydroxide nanohybrids with controlled release rate. *Chem Mater* **19**, 2679 (2007)
29. Sparks, DL: Kinetics of Soil Chemical Processes. Harcourt Jovanovich, San Diego (1989)

30. Uddin, MJ, Mondal, D, Morris, CA, Lopez, T, Diebold, U, Gonzalez, RD: An in vitro controlled release study of valproic acid encapsulated in a titania ceramic matrix. *App. Surf. Sci.* **257**, 7920 (2011)
31. Uddin, MJ, Islam, MA, Haque, SA, Hasan, S, Amin, MSA, Rahman, MM: Preparation of nanostructured TiO₂-based photocatalyst by controlling the calcining temperature and pH. *Int. Nano. Lett.* **2**, 19 (2012)
32. Venkatesha, R, Balachandaran, K, Sivaraj, R: Synthesis and characterization of nano TiO₂-SiO₂: PVA composite-a novel route. *Int. Nano. Lett.* **2**, 15 (2012)
33. Birks, LS, Friedman, H: Particle size determination from X-ray line broadening. *J. Appl. Phys.* **17**, 687 (1946)
34. Uddin, MJ, Cesano, F, Scarano, D, Bordiga, S, Zecchina, A: Effect of Ag and Au doping on the photocatalytic activity of TiO₂ supported on textile fibres. *Mater. Res. Soc. Symp. Proc.* **1077**, L07 (2008)
35. Lee, C, Sung, YW, Park, JW: Multiple equilibria of phenothiazine dyes in aqueous cyclodextrin solutions. *J. Phys. Chem. B.* **103**, 893 (1999)
36. Lachheb, H, Puzenat, E, Houas, A, Ksibi, M, Elaloui, E, Guillard, C, Herrmann, J-M: Photocatalytic degradation of various types of dyes (Alizarin S, Crocein Orange G, Methyl Red, Congo Red, Methylene Blue) in water by UV-irradiated titania. *App. Catal. B: Environ.* **39**, 75 (2002)
37. Zalazar, CS, Martin, CA, Cassano, AE: Photocatalytic intrinsic reaction kinetics. II: Effects of oxygen concentration on the kinetics of the photocatalytic degradation of dichloroacetic acid. *Chem. Eng. Sci.* **60**, 4311 (2005)
38. Hirakawa, T, Koga, C, Negishi, N, Takeuchi, K, Matsuzawa, S: An approach to elucidating photocatalytic reaction mechanisms by monitoring dissolved oxygen: Effect of H₂O₂ on photocatalysis. *App. Catal. B: Environ.* **87**, 46 (2009)
39. Liming, Y, Liya, EY, Madhumita, BR: Degradation of paracetamol in aqueous solutions by TiO₂ photocatalysis. *Water. Res.* **42**, 3480 (2008)
40. Dalrymple, OK, Yeh, DH, Trotz, MA: Removing pharmaceuticals and endocrine-disrupting compounds from wastewater by photocatalysis. *J. Chem. Tech. Biotech.* **82**, 121 (2007)
41. Sakkas, VA, Calza, P, Medana, C, Villioti, AE, Baiocchi, C, Pelizzetti, E, Albanis, T: Heterogeneous photocatalytic degradation of the pharmaceutical agent salbutamol in aqueous titanium dioxide suspensions. *Appl. Catal. Environ.* **77**, 135 (2007)
42. Waed, A, Mahmoud, A: Kinetic study on photocatalytic degradation of several pharmaceuticals assisted by SiO₂/TiO₂ catalyst in solar bath system. *Jordan J. Pharma. Sci.* **3**, 121 (2010)

doi:10.1186/2228-5326-3-16

Cite this article as: Uddin *et al.*: Tailoring the photocatalytic reaction rate of a nanostructured TiO₂ matrix using additional gas phase oxygen. *International Nano Letters* 2013 **3**:16.

Submit your manuscript to a SpringerOpen[®] journal and benefit from:

- Convenient online submission
- Rigorous peer review
- Immediate publication on acceptance
- Open access: articles freely available online
- High visibility within the field
- Retaining the copyright to your article

Submit your next manuscript at ► springeropen.com
